TELKOMNIKA Telecommunication Computing Electronics and Control
Vol. 22, No. 5, October 2024, pp. 1073~1082
ISSN: 1693-6930, DOI: 10.12928/TELKOMNIKA.v22i5.26077

Graphene based terahertz patch antenna for breast tumor detection

Lia Moni, Md. Saniat Rahman Zishan, Sumit Hassan Eshan, Raja Rashidul Hasan
Department of Electrical and Electronic Engineering, Faculty of Engineering, American International University-Bangladesh (AIUB), Dhaka, Bangladesh

Article Info

Article history:

Received Feb 13, 2024
Revised May 12, 2024
Accepted May 26, 2024

Keywords:

2D materials
Breast tumor
Graphene
Return loss
Terahertz

ABSTRACT

Breast cancer is a potentially life-threatening disease is one of the most common cancers specially for women. For fast and effective treatment early detection of the tumor is very important. But the frequent checkup is not possible for many people with the traditional way of detection due to their cost and availability. To detect the biomedical imaging terahertz (THz) frequency is a suitable range and using patch antenna in biomedical detection is cost effective compared to the traditional methods. So, to detect the early stage of breast tumor, this article has proposed a graphene based THz antenna. The primary goal of this antenna is to detect the breast tumor with the improvement of the performance and the secondary goal is to make the antenna very light weighted. The design of the antenna was done using computer simulation technology (CST) studio and the dimension of the antenna is kept 18×23 μm^2 and a breast phantom model has been designed and the performance analysis of the antenna has been done for both free space and breast tissue. The return loss of the antenna in free space is -52.4422 dB at 6.96 THz. The details of the detection of tumor through the proposed patch antenna has been shown in this study.

Corresponding Author:

Lia Moni
Department of Electrical and Electronic Engineering, Faculty of Engineering
American International University-Bangladesh (AIUB)
Dhaka, Bangladesh
Email: 22-92768-3@student.aiub.edu

1. INTRODUCTION

In contemporary times, cancer has emerged as a formidable global health challenge. According to the world health organization (WHO) in 2019, cancer ranked as the foremost or secondary cause of mortality in 112 out of 183 countries, assuming the third or fourth position in the remaining nations. Projections intimated an alarming expectation of 19.3 million new cancer cases and 10 million cancer-related fatalities by 2020 [1]. Analysis of global cancer statistics (GLOBOCAN) 2020 data, as presented by the International Agency for Research on Cancer (IARC), reflected an augmentation, with 2,261,419 cases and 684,996 deaths, comprising 11.7% and 6.9%, respectively, of the total 35 cases. Notably, breast cancer exhibited the highest incidence and mortality rates among the 35 identified cancers. The disconcerting statistic elucidated that 1 in 4 women is at risk of developing breast cancer, with 1 in 8 succumbing to the ailment [2]. Given its elevated mortality rate, the imperative of early detection for breast tumors or cancer cannot be overstated. A gamut of methodologies, including ultrasound, X-ray mammograms, and magnetic resonance imaging (MRI), are deployed for detection but they are expensive for frequent checkup. Therefore, employing a microstrip patch antenna can serve as a viable alternative for early detection of the tumor ensuring minimal impact on the human body [3]. So, this study aimed to develop a lightweight antenna designed for high-frequency operation, with a specific focus on

its application in biomedical scenarios, particularly the early detection of breast cancer. The choice of a patch antenna was motivated by its advantageous features, including low weight, thin profile, and support for both linear and circular polarization [3]. Given the goal of operating within a high-frequency band, the terahertz (THz) range was selected. In terms of material selection for the antenna patch, graphene was opted for, despite the availability of various traditional materials for patch antennas [4]. The reasons of chosing graphene as patch materials and frequency as THz frequency are discussed below providing a foundation for the deliberate selection of a low-weight, high-frequency patch antenna tailored for the early-stage detection of breast cancer in biomedical applications.

The THz electromagnetic waves, encompassing the frequency range of 0.1-10 THz and wavelengths spanning 0.03-3 mm, are commonly utilized. In adherence to the IEEE standard, the designated frequency range of 0.3-10 THz is specifically allocated for THz waves [5]. Characterized by a minimal damage trait, THz waves exhibit lower single-photon energy compared to X-rays. This inherent safety renders them valuable in biomedical applications, such as detecting various cancer tissues for medical diagnostics. The employment of antennas for signal carrier communication in the THz wave holds the potential to significantly elevate data transfer rates, potentially reaching terabits per second [5], [6]. Due to the numerous advantages of THz technology, it has emerged as a highly favorable choice for researchers.

In the early 20s, the first successful process of exfoliating 2D materials took place [7]. 2D materials belong to the category of nanomaterials and possess dimensions along both the X and Y axes so have a thickness at the atomic scale [8]. With the potential to exhibit both complexity and elemental characteristics, they showcase distinctive mechanical, chemical, and optical properties such as, tunability of bandgap, higher conductivity and thermal stability. This paper focuses on graphene as the chosen 2D material, being the first successfully exfoliated material of its kind. Graphene, composed of carbon, features a hexagonal structure reminiscent of a honeycomb [9]. Graphene exhibits an impressive electron mobility exceeding 200,000 cm^2/V_S at 25 °C. Graphene-based devices with cutoff frequencies in the THz region are enabled by the elevated carrier mobility of material. Its remarkable capability to carry ultra-high current densities, reaching 1×10^9, is complemented by a thermal conductivity of 5×10^3 W/mK. The necessity for high power to overcome propagation losses in the environment and scattering losses in metal further limits the data transfer range. In contrast, graphene-based antennas with dimensions on the order of a few micrometers provide an alternative, as they can radiate in the THz communication band, showcasing the potential to address the limitations associated with metallic antennas [10].

In the domain of biomedical applications, microstrip patch antennas have gained prominence. Various types of detection methodologies have been explored using microstrip patch antennas. Aloui *et al*. [11] proposed a THz antenna for breast tumor detection, incorporating graphene as the primary material. Both the graphene and copper antennas exhibited an S11 parameter near -27.5 dB at a frequency of 4.6 THz. Hasan *et al*. [12] designed a patch antenna for gigahertz (GHz) range, showcasing S11 parameters of -49.92 dB in free space, -48.52 dB in normal lungs, -40.12 dB for 2 mm fluid in COVID-affected lungs, and -39.95 dB for 5 mm fluid. Study by [13] has proposed a micro-scaled graphene-based antenna with dimensions of 130×100 μm^2. The S11 parameter measured -19.49 dB which suitable for biomedical imaging and sensing applications in the THz region. Shalini and Madhan [14] introduced a compact multi-band graphene-based patch antenna for THz applications, radiating at 1.96 THz and 4.83 THz. The antenna exhibited return losses of -34 dB and -38 dB, with bandwidths of 80 GHz and 100 GHz, respectively. Goswami and Rahman [15] has designed a wideband off-body patch antenna for biomedical applications which is copper-based with dimensions of 38×25 mm^2. Hasan *et al*. [3] proposed an antenna based on multiwalled carbon nanotube (MWCNT) for breast cancer detection. With dimensions of 30×40 mm^2, the antenna exhibited a return loss of -33.414 dB in free space, -32.64 dB in normal breast tissue, and -34.94 dB in normal tumor tissue. Hlali *et al*. [16], has introduced the numerical simulation of a THz sensor composed of a patch antenna. The antenna size was 103×32 μm^2, with an S11 parameter of -22.5 dB. Azman *et al*. [17] fabricated a 24×46 mm^2 graphene-based antenna on Rogers technology or RT duroid substrate, achieving measured hardware and software S11 values of -17.6314 dB and -18.05 dB, respectively, with bandwidths of 0.156 GHz and 0.2974 GHz. Moulfi *et al*. [18] designed an optical nano-patch antenna with a size of 24×24 μm^2. The results for the graphene-based patch antenna on RO3003 substrate demonstrated maximum gain and bandwidth, with an S11 of -33.692 dB at 7.001 THz. Azani and Abidin [19] has proposed a THz microstrip patch antenna for breast tumor detection with dimensions of 200×200 μm^2, featuring an S11 of -25 dB at 0.35 THz. Anand *et al*. [20] designed a graphene nano-ribbon-based THz antenna with dimensions of 208.98×433.2 μm^2 and a return loss of -36 dB, constructed on a polyimide substrate.

2. METHOD

Computer simulation technology (CST) studio was utilized for the design of the antenna aimed at detecting breast tumors where graphene was opted for as the patch material. A key emphasis of the research

was to develop a lightweight antenna so size of the antenna was established at 23×18 μm^2, aligning with the goal of achieving a compact and efficient design suitable for breast tumor detection. The proposed antenna operates within the frequency range of 2 THz to 10 THz. Achieving the desired performance necessitated iterative adjustments to the length, thickness, and width of the antenna. Subsequently, a breast model phantom was fabricated, and various tumor shapes were incorporated to analyze the outcomes. The detection procedure was then conducted based on the findings derived from the analysis. During the material selection process for the antenna, utmost care was taken to ensure that the chosen materials are not harmful to the human body. The specifics of the work are outlined in Figure 1 via the flowchart.

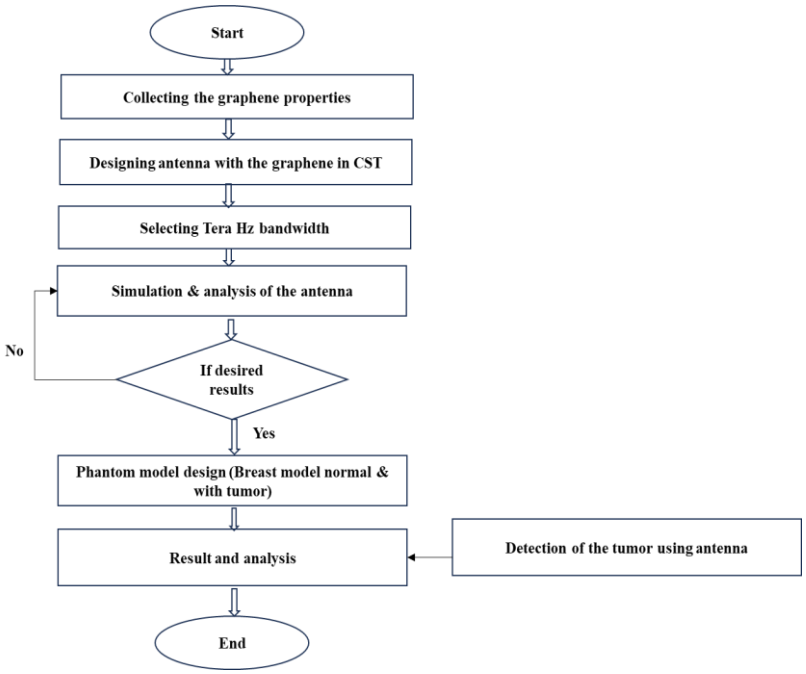

Figure 1. Flowchart of the work

2.1. Modelling of the graphene

Graphene provides favorable conditions for the propagation of surface plasmon polariton (SPP) waves and supports SPP in transverse magnetic (TM) mode. The dispersion relation for SPP in an air dielectric medium can be represented as (1) [21]:

$$-i\frac{\sigma_\omega}{\omega\varepsilon_0} = -\frac{1}{\sqrt{k_{spp}^2-\frac{\omega^2}{c^2}}} + \frac{\varepsilon_r}{\sqrt{k_{spp}^2-\frac{\omega^2}{c^2}\varepsilon_r}} \quad (1)$$

σ_ω = conductivity of the graphene
k_{spp} = SPP wave number= $k_0(\eta_{eff})$

The conductivity of the graphene can be expressed as the sum of the intra band and inter band conductivity of the graphene [10]:

$$\sigma_\omega = \sigma_{inter} + \sigma_{intra} \quad (2)$$

the contribution arising from the interband:

$$\sigma_{inter}(\omega) = \frac{e^2}{4\hbar}\left(H\left(\frac{\omega}{2}\right) + i\frac{4\omega}{\pi}\int_0^\infty \frac{H(\varepsilon)-H\left(\frac{\omega}{2}\right)}{\omega^2-4\varepsilon^2}\,\partial\varepsilon\right)\sigma_\omega = \sigma_{inter} + \sigma_{intra} \quad (3)$$

$$H(\varepsilon) = \frac{sinh\left(\frac{\hbar\varepsilon}{K_BT}\right)}{cosh\left(\frac{\mu_C}{k_BT}\right)+\cosh\left(\frac{\hbar C}{K_BT}\right)} \quad (4)$$

the contribution arising from the intraband:

$$\sigma_{intra}(\omega) = \frac{2e^2 K_B T i}{\pi\hbar^2(\omega + i\tau^{-1})} \ln = \left(2\, cosh\left(\frac{\mu_C}{2k_B T}\right)\right) \quad (5)$$

At THz frequencies where the Fermi level (EF) greatly exceeds the photon energy ($\hbar\omega$) and the interband conductivity of graphene is considered negligible compared to the intraband conductivity. In this regime, the drude-like intraband conductivity predominates, as stated in reference [10]. Consequently, the graphene conductivity can be expressed as (6):

$$\sigma_{\omega} = \frac{2e^2 K_B T i}{\pi\hbar^2(\omega + i\tau^{-1})} \ln = \left(2\, cosh\left(\frac{\mu_C}{2k_B T}\right)\right) \quad (6)$$

2.2. Modelling of the antenna

During the initial phases of antenna design, computations were conducted utilizing the formulas referenced in [22]. These computations facilitated the determination of dimensions required to define the antenna patch. Formula-1 is utilized to compute the width of the patch:

$$w = \frac{c}{2f_0\sqrt{\frac{\varepsilon_r + 1}{2}}} \quad (7)$$

Formula-2 is employed to determine the length the width of the patch.

$$L = \frac{c}{2f_0\sqrt{\frac{\varepsilon_r + 1}{2}}} - 0 \cdot 824h\left\{\frac{\left(\varepsilon_{reff} + 0.3\right)\left(\frac{\omega}{h} + 0{\cdot}264\right)}{\left(\varepsilon_{reff} - 0.258\right)\left(\frac{\omega}{h} + 0{\cdot}8\right)}\right\} \quad (7)$$

Figure 2 illustrates the model of the antenna and body phantom created in CST studio. In Figure 2(a), the antenna dimensions are depicted, while Figure 2(b) provides a three-dimensional view of the antenna, segmented into three parts: the ground, substrate, and patch. Copper serves as the material for the ground, and flame retardant 4 (FR4) with a dielectric constant of 4.8 is chosen for the substrate, while graphene, a 2D material, is selected for the patch. Figure 2(c) displays the antenna port connected at the bottom of the antenna, and Figure 2(d) showcases the breast phantom model, featuring a section of the breast where three basics layers are shown for a normal breast. In Table 1 the specification of the antenna is mentioned. In Table 2 the specification of the breast phantom is mentioned [3].

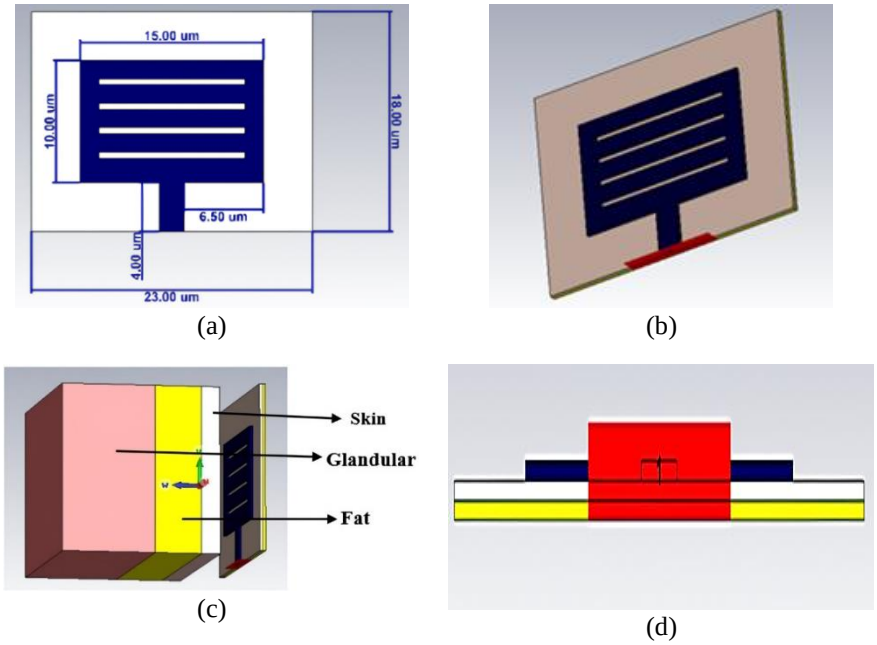

Figure 2. Design of the antenna: (a) dimension of the antenna, (b) 3d view of graphene-based patch antenna, (c) a portion of breast phantom, and (d) port of the antenna

Table 1. Parameters of antenna

Parameters	Size (micrometer)	Parametrs	Size	Paramets	Size
Ground length (Gl) = *Substrate length* (Sl)	18	Pl1	4	Pw2	15
Ground width (Gw) = ***Substrate*** *width* $(\boldsymbol{Sw})$	23	Pw1	2	Pt	0.3
Ground thickness(Gt) = *Substrate thickness* (St)	0.3	Pl2	8		

Table 2. Parameters of the breast phantom

	Permeability	Electric conductivity	Density	Thermal conductance	Diffusivity
Skin	34.946	3.8912	1100	0.50	7.6×10^{-8}
Fat	4.9367	0.30623	910	0.24	8.8×10^{-8}
Glandular	-	3.46	1041	33	1.07×10^{-5}
Tumor	54.9	4	1058	-	-
Tumor with cancer	7052	26	-	-	-

3. RESULTS AND DISCUSSION

3.1. Antenna in free space

The antenna is constructed with careful consideration to uphold a 50 Ω impedance match. This decision is pivotal as it secures efficient power transfer between the transmitter and the antenna, minimizing power losses and optimizing signal transmission. This adherence to impedance matching also guarantees compatibility with other radio frequency (RF) components designed for a 50 Ω impedance. Figure 3(a) shows the impedance matching of the desired antenna where the impedenace matching is done at 50 Ω. For any operating antenna, the return loss value must be less than -10 dB [3], [22]. Here, Figure 3(b) depicts the return loss of the antenna in free space, indicating a minimum S11 value of -52.4422 dB at 6.96 THz. Additionally, a voltage standing wave ratio (VSWR) value between 1 to 2 is considered acceptable, with an ideal value being one [22]. Figure 3(c) illustrates the VSWR value of the antenna in free space, registering at 1.0047858 THz at 6.96 THz which is very close to the ideal value. Figure 3(d) exhibits the three-dimensional far-field pattern of the antenna in a free space. This representation reveals that both radiation efficiency and total efficiency measure -21.35 dB and -21.36 dB, correspondingly, with a directivity of 5.294 dBi at 6.96 THz. Meanwhile, Figure 3(e) illustrates the polar far-field pattern of the antenna in free space, depicting a primary lobe magnitude of 5.29 dBi. The angular span of the primary lobe is 98.1°, positioned at main lobe direction of 19°. The numbers 5.29 dBi tell us how strong the signal is in that main direction, and the 98.1° angle shows how wide the area is that the signal covers. The main lobe direction at 19° indicates where the antenna focuses most of its signal.

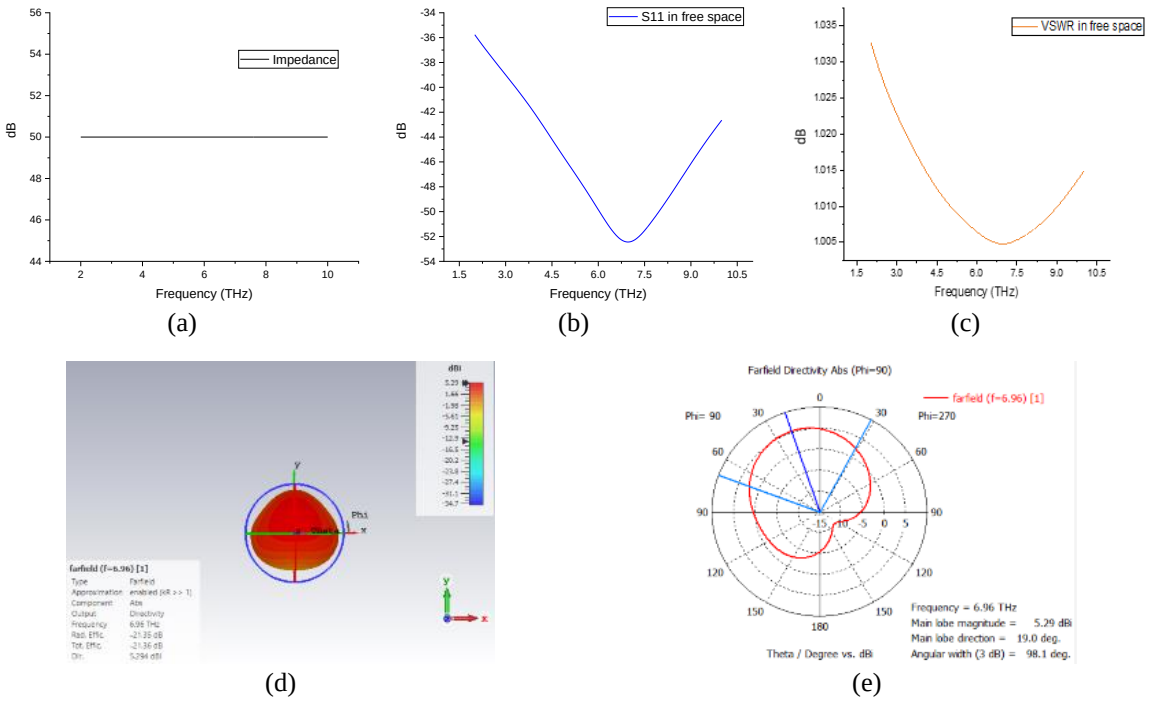

Figure 3. Antenna performane criteria: (a) reference impedance of the antenna, (b) S11 in free space, (c) VSWR in free space, (d) directivity in free space, and (e) directivity in polar in free space

3.2. Antenna in normal breast

Figure 4(a) presents the return loss of the antenna when placed in a normal breast environment, revealing a minimal S11 value of -51.187344 dB at 6.424 THz which less than -10 dB. So, it can be stated that the antenna can operate in normal breast. Moreover, the VSWR value of the antenna in the normal breast scenario is depicted in Figure 4(b), recorded at 1.0055317 THz at 6.424 THz which is also near to the ideal value. Figure 4(c) showcases the three-dimensional far-field pattern of the antenna within a normal breast environment. This visual representation elucidates that the radiation efficiency and total efficiency are measured at -17.36 dB and -17.37 dB, respectively, with a directivity of 6.424 dBi at 6.424 THz. Concurrently, Figure 4(d) displays the polar far-field pattern, highlighting a primary lobe magnitude of 6.32 dBi. The angular breadth of the primary lobe spans 58.1°, positioned at an inclination of 8°.

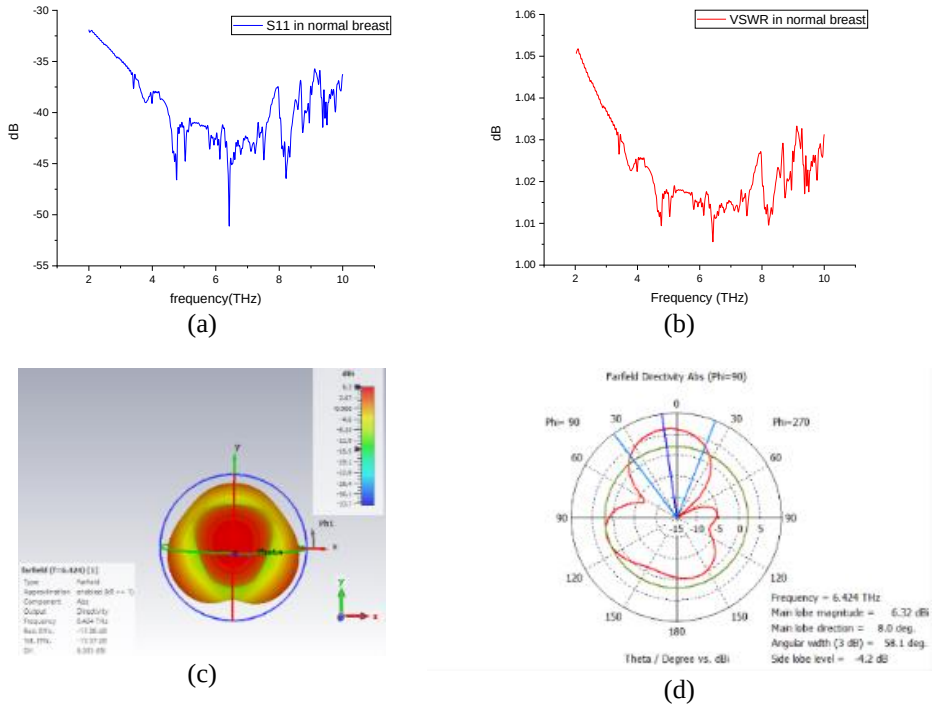

Figure 4. Antenna performane criteria with breast phantom: (a) S11 in normal breast, (b) VSWR in normal breast, (c) directivity in normal breast, and (d) directivity in polar in normal breast

3.3. For different size of the tumor

The Figure 5 shows the different tumor sizes in breast phantom and the effect of return losses for those particular tumors. Figure 5(a) presents the segment of breast phantom model with 2 mm tumor, Figure 5(b) represents the breast phantom model with 3 mm tumor and Figure 5(c) represents the breast model with 4 mm tumor. Figure 5(d) represents the comparison of the return losses for three different sizes of the tumors.

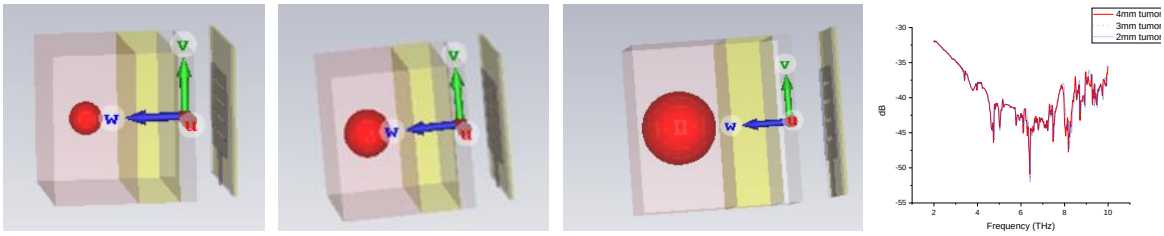

(a) (b) (c) (d)

Figure 5. Phantom model with different tumor sizes: (a) phantom of breast with 2 mm tumor, (b) phantom of breast with 3 mm tumor, (c) phantom of breast with 4mm tumor, and (d) return losses of the antenna for different size of the tumors

Table 3 depicts the performances of the antenna for different sizes of the tumor. The observation from the table reveals that when the tumor size is 2 mm, the resonant frequency remains constant, but the return loss shifts to -51.95 dB. Upon increasing the tumor size to 2 mm, both the resonant frequency and return loss change, with the frequency shifting to 6.416 THz and the return loss to -52.006 dB. Furthermore, with a tumor size of 3 mm, there is another shift in the resonant frequency, accompanied by a return loss of -50.9 dB. The directivity and VSWR of the antenna also changes for different sizes of the tumor which are shown on Table 3. This indicates that as the tumor size increases, both the resonant frequency and return loss exhibit greater shifts. As the antenna can operate effectively and provide distinct data corresponding to various sizes of tumors, it has the capability to detect tumors of different sizes.

Table 3. Antenna performance for different size of the tumor

Tumor size	Resonant frequency (THz)	Return loss (S11) (dB)	VSWR	Directivity (dBi)
2 mm	6.424	-51.95	1.0050646	6.424
3 mm	6.416	-52.006	1.0050326	6.335
4 mm	6.4	-50.900	1.0057177	5.951

3.4. For different position of the tumor

Figure 6 depicts variations in the phantom breast model corresponding to different tumor positions. Figure 6(a) presents the segment of breast phantom model when the tumor is at position-1, Figure 6(b) represents the breast phantom model where tumor is at position-2 and Figure 6(c) represents the breast model with a tumor positioned at 3. Figure 6(d) represents the comparison of the return losses for three different positions of the tumors.

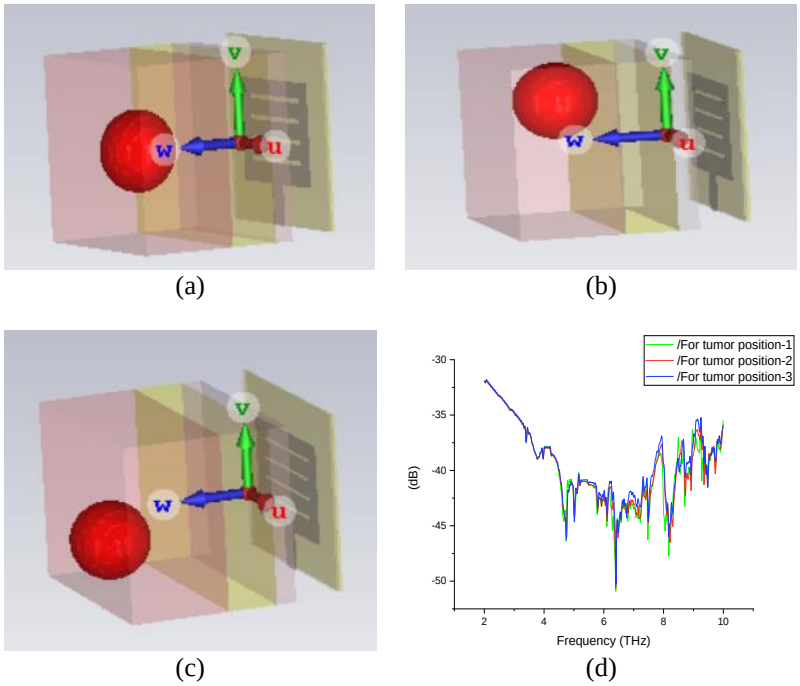

Figure 6. Phantom model with different tumor positions: (a) tumor at position-1, (b) tumor at position-2, (c) tumor at position-3, and (d) return losses of the antenna for different position of the tumors

Table 4 illustrates the performances of the antenna for various tumor positions. The data indicates that when the tumor is located at position-1, the resonant frequency is 6.4 THz, accompanied by a return loss of -50.9 dB. Shifting the tumor to position-2 results in a return loss of -50.6184 dB at a resonant frequency of 6.416 THz. Similarly, at position-3 of the tumor, the antenna exhibits a return loss of -50.2729 dB with a resonant frequency of 6.408 THz. VSWR and the directivity of the antenna also changes for different sizes of the tumor which are shown on Table 4. As the antenna can operate effectively and provide distinct data corresponding to various sizes of tumors, it has the capability to detect tumors at different positions.

Table 4. Antenna performance for different position of the tumor

Tumor position no	Resonant frequency (THz)	Return loss (S11) (dB)	VSWR	Directivity (dBi)
1	6.4	-50.900	1.0057177	5.951
2	6.416	-50.6184	1.00509073	6.562
3	6.408	-50.2729	1.0061477	6.009

From the performance of of the antenna across diverse environments, it is evident that the antenna operates in different environments with the shifting of the resonant frequency as well as ensuring different return losses. Initially, resonant frequency of the antenna measured at 6.96 THz in free space. However, upon placement near a normal breast tumor, the resonance frequency shifted to 6.424 THz, accompanied by a change in the S11 parameter from -52.44 to -51.18 dB. Subsequently, when positioned near a tumor-affected breast, the resonance frequency further adjusted to 6.4 THz, with an S11 value of -50.9 dB. Finally, when exposed to a cancerous tumor, the frequency shifted again, this time to 9.712 THz, with an S11 value of -46.58 dB. The directivity of the antenna was 5.294 dBi at free space but it changes the directivity at normal breast phantom and becomes 6.32 dBi. In a normal breast phantom, the directivity increased to 6.32 dBi. For a tumor-affected breast, the directivity shifted to 5.951 dBi, and for a cancerous tumor-affected breast, it further increased to 7.557 dBi. Despite these changes, the VSWR value showed slight fluctuations across various environments but consistently remained close to the ideal value. This versatility underscores the potential efficacy of the antenna in detecting breast tumors, as it effectively responds to environmental variations, showcasing promising sensitivity to tumor presence.

Table 5 compiles studies on THz antennas, detailing their dimensions, applications, and patch materials. Upon thorough analysis of the data in the table, it's evident that the proposed antenna stands out for its lightweight design, measuring 18×23 μm^2, which is smaller than other works mentioned. Additionally, the proposed antenna exhibits lower return loss compared to the referenced works, indicating better matching with the transmission line. These characteristics contribute to the exceptional performance of the proposed antenna, particularly in tumor detection, highlighting its superiority over existing studies in the field.

Table 5. Comparison of the antenna

Antenna size	Patch material	Substrate material	Resonance frequency (THz)	S11 (dB)	Applications	Ref
40×30 mm^2	MWCNT	Rogger	0.078/0.076/0.07064	-33.414/ -32.6/35.22	Breast cancer detection	[3]
15×21 μm^2	Graphene	Duroid	4.6	-27.5	Breast tumor-detection	[11]
80×80 mm^2	MWCNT	FR4	0.0729	-47.92/ -48.52/-40.12	Detecting COVID-19-affected lungs	[12]
130×100 μm^2	Graphene	RogersRT/Duroid 6010™	0.795	-19.49	THz applications	[13]
50×50 μm^2	Graphene	Silicon-di-oxide	1.96/4.83	-34/-38	Multi-band operation	[14]
110×103 μm^2	Graphene	Duroid	0.859/0.902/0.93	-22/~-21 ~24	Breast tumor detection	[16]
200×200 μm^2	Graphene	Polyimide	0.35	-25(free space)	Breast tumor detection	[19]
40×40 μm^2	Graphene	Silicon	1.79	-42.3	THz communications	[23]
40×40 μm^2	Graphene	FR4	4.79	-13.7875	THz application	[24]
532×500 μm^2	Graphene	Quartz	1.06	-38.6	UWB applications	[25]
65×65 μm^2	Graphene	Silicon-di-oxide	1.96/4.83	-34/-38	THz applications	[26]
18×23 μm^2	Graphene	FR4	6.96/6.424/6.4/9.712	-52.4422/-51.187/-50.9/-46.58	Breast tumor detection	Proposed work

Given the considerations of availability and cost-effectiveness associated with breast tumor detection methods, the proposed antenna design seeks to address these challenges. The primary objective of this study is to maximize antenna performance, particularly for the early-stage detection of breast tumors which have been done successfully by using graphene as patch material in THz region. Looking ahead, if the proposed antenna can be successfully fabricated and validated. Through testing, it holds the potential to surpass existing antenna designs in terms of performance. Its anticipated cost-effectiveness and compact size could prove instrumental in saving lives by facilitating the early detection of breast tumors. Overall, this study underscores the importance of innovative approaches in antenna design for advancing medical diagnostics, particularly in the context of breast cancer detection.

4. CONCLUSION

In this work, a graphene-based patch antenna has been presented that has a resonance frequency of 6.96 THz, operating in the THz band. The purpose of the antenna is to detect breast tumors in the human body. All aspects of the antenna, including operating frequency, return loss, VSWR, and radiation patterns, have been investigated in different environments. For the investigation, CST microwave studio has been used. The antenna operates at 6.96 THz, providing a return loss of -52.44 dB in free space. In a normal breast, the return loss is -51.18 dB with the shift of resonance frequency at 6.424 THz, whereas in a tumor-effected breast, the resonance frequency changes to 6.4 THz with a return loss of -50.9 dB. For cancerous tumors, the operating frequency changes to 9.712 THz with a return loss of -46.58 dB. So, it is evident that the designed antenna can operate very well, and the resonance frequency changes with the variation of the antenna. This research shows that it is possible to detect the breast tumor early which can contribute to saving the lives of people.

REFERENCES

[1] H. Sung *et al.*, "Global cancer statistics 2020: GLOBOCAN estimates of incidence and mortality worldwide for 36 cancers in 185 countries," *CA: A Cancer Journal for Clinicians*, vol. 71, no. 3, pp. 209–249, May 2021, doi: 10.3322/caac.21660.

[2] D. Kashyap *et al.*, "Global increase in breast cancer incidence: risk factors and preventive measures," *BioMed Research International*, vol. 2022, pp. 1–16, Apr. 2022, doi: 10.1155/2022/9605439.

[3] R. R. Hasan *et al.*, "Spin coated multi-walled carbon nanotube patch antenna for breast cancer detection," *Advanced Materials Technologies*, vol. 8, no. 24, 2023, doi: 10.1002/admt.202300822.

[4] A. E. Fatimi, S. Bri, and A. Saadi, "UWB antenna with circular patch for early breast cancer detection," *Telecommunication Computing Electronics and Control*, vol. 17, no. 5, pp. 2370–2377, Oct. 2019, doi: 10.12928/TELKOMNIKA.v17i5.12757.

[5] Y. He, Y. Chen, L. Zhang, S. W. Wong, and Z. N. Chen, "An overview of terahertz antennas," *China Communications*, vol. 17, no. 7, pp. 124–165, Jul. 2020, doi: 10.23919/J.CC.2020.07.011.

[6] S. Abadal, S. E. Hosseininejad, A. Cabellos-Aparicio, and E. Alarcón, "Graphene-based terahertz antennas for area-constrained applications," in *International Conference on Telecommunications and Signal Processing*, Jul. 2017, pp. 817–820, doi: 10.1109/TSP.2017.8076102.

[7] Q. Ma, G. Ren, K. Xu, and J. Z. Ou, "Tunable optical properties of 2D materials and their applications," *Advanced Optical Materials*, vol. 9, no. 2, Jan. 2021, doi: 10.1002/adom.202001313.

[8] Y. Seekaew and C. Wongchoosuk, "Introductory chapter: 2D materials," in *2D Materials*, IntechOpen, 2019.

[9] A. H. C. Neto, F. Guinea, N. M. R. Peres, K. S. Novoselov, and A. K. Geim, "The electronic properties of graphene," *Reviews of Modern Physics*, vol. 81, no. 1, pp. 109–162, Jan. 2009, doi: 10.1103/RevModPhys.81.109.

[10] M. A. K. Khan, T. A. Shaem, and M. A. Alim, "Graphene patch antennas with different substrate shapes and materials," *Optik*, vol. 202, p. 163700, Feb. 2020, doi: 10.1016/j.ijleo.2019.163700.

[11] R. Aloui, H. Zairi, F. Mira, I. Llamas-Garro, and S. Mhatli, "Terahertz antenna based on graphene material for breast tumor detection," *Sensing and Bio-Sensing Research*, vol. 38, p. 100511, Dec. 2022, doi: 10.1016/j.sbsr.2022.100511.

[12] R. R. Hasan, A. M. Saleque, A. B. Anwar, M. A. Rahman, and Y. H. Tsang, "Multiwalled carbon nanotube-based on-body patch antenna for detecting COVID-19-affected lungs," *ACS Omega*, vol. 7, no. 32, pp. 28265–28274, Aug. 2022, doi: 10.1021/acsomega.2c02550.

[13] M. Krishna Ch, T. Islam, N. Suguna, S. V. Kumari, R. D. H. Devi, and S. Das, "A micro-scaled graphene-based wideband (0.57–1.02 THz) patch antenna for terahertz applications," *Results in Optics*, vol. 12, p. 100501, Jul. 2023, doi: 10.1016/j.rio.2023.100501.

[14] M. Shalini and M. G. Madhan, "Performance predictions of slotted graphene patch antenna for multi-band operation in terahertz regime," *Optik*, vol. 204, p. 164223, Feb. 2020, doi: 10.1016/j.ijleo.2020.164223.

[15] N. Goswami and M. A. Rahman, "A 9.73 GHz wide-band off-body patch antenna for biomedical applications," *Indonesian Journal of Electrical Engineering and Computer Science*, vol. 33, no. 1, p. 151, Jan. 2024, doi: 10.11591/ijeecs.v33.i1.pp151-158.

[16] A. Hlali, A. Oueslati, and H. Zairi, "Numerical simulation of tunable terahertz graphene-based sensor for breast tumor detection," *IEEE Sensors Journal*, vol. 21, no. 8, pp. 9844–9851, Apr. 2021, doi: 10.1109/JSEN.2021.3060326.

[17] N. I. Z. Azman, M. K. Othman, N. A. A. Zaini, and M. A. Jusoh, "Graphene-based materials for microstrip patch antenna," *Progress In Electromagnetics Research C*, vol. 126, pp. 207–216, 2022, doi: 10.2528/PIERC22090505.

[18] B. Moulfi, S. Ferouani, and Z. K. Djalal, "Optical nano patch antenna for terahertz applications with graphene," *Revista Mexicana de Fisica*, vol. 69, no. 6, Nov. 2023, doi: 10.31349/RevMexFis.69.061302.

[19] M. A. S. Md Azani and Z. Z. Abidin, "Terahertz microstrip patch antenna for breast tumour detection," *Journal of Electronic Voltage and Application*, vol. 4, no. 1, Oct. 2023, doi: 10.30880/jeva.2023.04.01.006.

[20] S. Anand, D. S. Kumar, R. J. Wu, and M. Chavali, "Graphene nanoribbon based terahertz antenna on polyimide substrate," *Optik*, vol. 125, no. 19, pp. 5546–5549, Oct. 2014, doi: 10.1016/j.ijleo.2014.06.085.

[21] S. A. Khaleel, E. K. I. Hamad, N. O. Parchin, and M. B. Saleh, "MTM-inspired graphene-based THz MIMO antenna configurations using characteristic mode analysis for 6G/IoT applications," *Electronics (Switzerland)*, vol. 11, no. 14, p. 2152, Jul. 2022, doi: 10.3390/electronics11142152.

[22] M. S. Rana, T. A. Fahim, S. B. Rana, R. Mahbub, and M. M. Rahman, "Design, simulation, and analysis of microstrip patch antenna for wireless applications operating at 3.6 GHz," *Telecommunication Computing Electronics and Control*, vol. 21, no. 5, pp. 957–967, 2023, doi: 10.12928/TELKOMNIKA.v21i5.24813.

[23] M. Dashti and J. D. Carey, "Graphene microstrip patch ultrawide band antennas for THz communications," *Advanced Functional Materials*, vol. 28, no. 11, p. 1705925, 2018, doi: 10.1002/adfm.201705925.

[24] S. P. J. Christydass, J. Suganthi, S. Kavitha, and R. Yuvaraj, "Ring monopole antenna for tera-hertz application," *Materials Today: Proceedings*, vol. 45, pp. 1827–1833, 2021, doi: 10.1016/j.matpr.2020.09.003.

[25] S. Asha, K. R. Shanthy, and S. K. Kumari, "Graphene based rectangular microstrip patch antenna for UWB applications," *Journal of Physics: Conference Series*, vol. 2484, no. 1, p. 012046, May 2023, doi: 10.1088/1742-6596/2484/1/012046.

[26] M. Shalini and M. G. Madhan, "Design and analysis of a dual-polarized graphene based microstrip patch antenna for terahertz applications," *Optik*, vol. 194, p. 163050, Oct. 2019, doi: 10.1016/j.ijleo.2019.163050.

BIOGRAPHIES OF AUTHORS

Lia Moni received her Bachelor of Science degree in Electrical and Electronic Engineering (EEE) in 2022 from American International University-Bangladesh (AIUB). She is currently pursuing her Master of Science in Electrical and Electronic Engineering (EEE) from AIUB. She has started working as a teaching assistant in the Faculty of Engineering at AIUB on October 2022. The areas of her research focus include renewable energy technology, 6G communications, 2D material-based antenna, energy harvesting antenna, and also biomedical engineering. She can be contacted at email: 22-92768-3@student.aiub.edu.

Md. Saniat Rahman Zishan received B.Sc. in Electrical and Electronic Engineering and Master of Engineering in Telecommunications degree from American International University-Bangladesh (AIUB). He completed Ph.D. from Universiti Sultan Zainal Abidin in the field of e-Health. On September 2009, he started his teaching career as a lecturer in AIUB. At present he is serving as an Associate Professor and Director of the Faculty of Engineering in the same university. He also worked as the Special Assistant of Office of Student Affairs (OSA) from December 2012 to till September 2018 and Head of Department of Computer Engineering (CoE) from September 2018 to till March 2023. He has published more than 50 articles in different journals and international and national level conferences. His research interest includes e-health, wireless communication, signal processing, telemedicine and robotics. He is a member of the Institute of Electrical and Electronics Engineers (IEEE) and Institution of Engineers, Bangladesh (IEB). He can be contacted at email: saniat@aiub.edu.

Sumit Hassan Eshan received the B.Sc. degree in Electrical and Electronic Engineering from American International University Bangladesh (AIUB), Dhaka, Bangladesh, in 2022.He passed his Higher Secondary School Certificate test in 2017 from Sheikh Amanullah Degree College, Kalaroa, Satkhira, as well as the Secondary School Certificate exam in 2015 from Kalaroa G.K.M.K. Pilot High School. Currently, he is working as a senior technical support engineer at the Microsoft and Cyber Security Department, Contessa Solutions and Consultants Ltd., Dhaka, Bangladesh. His research interests are in bio-implantable antenna design, RF antenna and propagation, optoelectronics, sensors, and nanomaterials. He is an expert antenna and filter designer using CST software. He has published 6 conference papers and 3 journal papers. He can be contacted at: sumithassaneshan@gmail.com.

Raja Rashidul Hasan received M.Sc. in Telecommunication and B.Sc. in Electrical and Electronic Engineering from American International University Bangladesh (AIUB), Dhaka, Bangladesh in 2012 and 2009 respectively. He has been an Assistant Professor, Faculty of Engineering, Department of Electrical and Electronic Engineering with American International University (AIUB) since 2013. He is interested in bio-implantable antenna design, RF antenna and propagation, optoelectronics, optical sensors and nanomaterials. He has 35 of publications among them 22 conferences, 12 journal papers and 1 book chapter internationally published. He can be contacted at email: hemal@aiub.edu.